GEOPHYSICAL RESEARCH LETTERS, VOL. 27, NO. 7, PAGES 1041-1044, APRIL 1, 2000

Evidence for shear velocity anisotropy in the lowermost mantle beneath the Indian Ocean

Jeroen Ritsema

Seismological Laboratory, California Institute of Technology, Pasadena

Abstract. Teleseismic recordings ($\Delta > 87°$) of a deep earthquake beneath the Banda Sea at stations in Tanzania show a difference in the arrival time of the radial (S^{SV}) and transverse component (S^{SH}) S wave ranging from 1–3 s. Shear velocity anisotropy in the lowermost mantle beneath the Indian Ocean is the likely cause of this signal because recordings at the same stations of closer–in events ($\Delta < 80°$) in the same source region do not present a comparable differential travel time. For the Banda Sea event, the S^{SH} signals are broader than S^{SV} signals, suggesting that a discontinuity (or strong vertical gradient) in primarily V_{SH} marks the sudden onset of transverse isotropy in D" (with a magnitude of 1.4–2.7%) about 350 km above the core–mantle boundary. SKKS coda, S–to–p converted phases at the Moho, and upper mantle heterogeneity beneath the stations obscure the onset of S^{SV} and complicate wave shapes. It is therefore difficult to evaluate whether general anisotropy needs to be invoked into a model of shear velocity anisotropy.

1. Introduction

Structure characterised by shear velocity anisotropy in the lowermost several hundred kilometers of the mantle (D") provides constraints on convective flow patterns in the deep mantle [e.g., *Kendall and Silver*, 1998; *Lay et al.*, 1998a]. Shear velocity anisotropy in D" is typically examined using models of transverse isotropy and quantified by the difference between the travel times of radial (S^{SV}) and transverse (S^{SH}) components S or ScS waves, denoted as T_{SSV_SSH}.

While the global compilation of *Dziewonski et al.* [1996] shows a symmetric distribution of T_{SSV_SSH} about zero, regional investigations present a systematic geographic pattern. Positive values of T_{SSV_SSH} (up to 5 s) are obtained for sampling regions of D" beneath Alaska [*Lay and Young*, 1991; *Matzel et al.*, 1996; *Garnero and Lay*, 1997], the Caribbean [*Kendall and Silver*, 1996], and the northeastern Pacific [e.g., *Vinnik et al.*, 1995; *Ritsema et al.*, 1998]. In these regions, the shear velocity is relatively high and strong vertical shear velocity gradients have been proposed [e.g., *Lay et al.*, 1998b]. Smaller values of T_{SSV_SSH}, ranging from -2 to +2 s, are observed for the D" region beneath the central Pacific [*Pulliam and Sen*, 1998; *Ritsema et al.*, 1998; *Russel et al.*, 1998] where, on average, the shear velocity is low.

Here, I present recordings of the August 30, 1994 Banda Sea earthquake at seismic stations in Tanzania which provide evidence for the presence of shear velocity anisotropy in D" beneath the Indian Ocean. These data corroborate previous suggestions that anisotropic structure in relatively high shear velocity D" regions yields positive values of T_{SSV_SSH} and that a strong vertical shear velocity gradient marks its upper boundary [e.g., *Lay and Young*, 1991; *Matzel et al.*, 1996].

2. Indonesia earthquake recordings

Recordings of deep-focus earthquakes allow for precise measurements of T_{SSV_SSH}. S waveforms from deep earthquakes are not complicated by the interference with surface reflections or affected by upper mantle anisotropy in the earthquake source region.

The 1994–1995 broadband deployment in Tanzania [*Nyblade et al.*, 1996] recorded three deep Indonesian earthquakes with body wave magnitudes larger than 5.7 (Table 1). These events are at identical easterly azimuth from the Tanzania Network and generated seismic shear waves that propagate to stations in Tanzania through the same mantle corridor (Figure 1). S waves generated by events A and B (Δ=71–80°) turn at least 700 km above the CMB. S waves generated by event C ($\Delta > 87°$), on the other hand, propagate through the uppermost regions of D" ($\approx$ 150–350 km above the CMB) where shear velocities are, on average, 1.5% higher than in the Preliminary Reference Earth Model (PREM) [*Dziewonski and Anderson*, 1981].

Figure 2 compares the highest quality S wave recordings for events A and C. The S^{SH} and S^{SV} signals of event A have similar onset times and wave shapes. The S waveform complexity, similar for S^{SH} and S^{SV}, may be caused by the strong lateral variation of seismic shear

Table 1. Event parameters.

	Event	Lat.(°S)	Lon.(°E)	Depth (km)
A	Sep 28, 1994	5.8	110.3	643
B	Nov 15, 1994	5.6	110.2	559
C	Aug 30, 1994	7.0	124.2	618

Copyright 2000 by the American Geophysical Union.

Paper number 1999GL011037.
0094-8276/00/1999GL011037$05.00

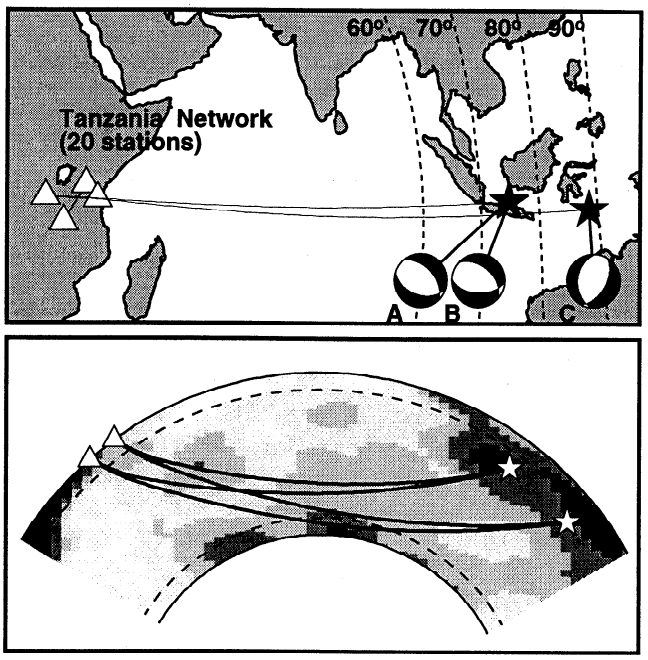

Figure 1. (top) Geographic map (mercator projection) centered on the Indian Ocean showing the epicenters (stars) and focal mechanisms of events A, B, and C (Table 1), and locations (triangles) of outermost stations of the Tanzania Network. The solid lines connect the epicenters to the center of the network, while the dashed lines are lines of equal distance (60°, 70°, and 80°) to the center of the network. (bottom) Vertical cross sections through model S20RTS [*Van Heijst et al.*, 1999] along the great circle path through the earthquake epicenters and the Tanzania Network. Shear velocity in regions with dark (light) grey shades are relatively high (low). The solid lines are geometrical ray paths of S computed for the PREM model. The dashed lines are horizons in the mantle at 300 km depth below the Earth's surface and 300 km above the CMB.

velocity in the crust and upper mantle beneath the East African Rift and Tanzania Craton [*Ritsema et al.*, 1998; *Ritsema and Van Heijst*, 2000].

The pronounced differences between S^{SH} and S^{SV} waveshapes for event C indicate that S wave propagation is strongly affected by structure in the lowermost mantle. At stations URAM, PUGE and MITU, S^{SH} is broader than S^{SV} and SKS and the S^{SH} pulse at station MTOR exhibits two distinct peaks. The presence of SKS signal on the transverse component recordings of event C at URAM, PUGE, and MTOR suggest that upper mantle anisotropy may, to some extend, be the cause of S waveform complexity. Models of upper mantle anisotropy described by the fast S wave polarisation angle (Φ_f) and the differential travel time between the fast and slow S wave (Δt) [e.g., *Silver*, 1996] can account for the SKS splitting at URAM and PUGE (but not MTOR). However, corrections for upper mantle anisotropy using such models do not remove the S^{SH} waveform complexity despite the fact the incidence angles of S and SKS differ by less than 10°. Low values (< 0.5 s) of Δt were also obtained by *Hill et al.* [1996] using SKS data for a worldwide distribution of earthquakes.

Ruling out upper mantle structure, the S^{SH} waveform complexity suggests that S^{SH} is interacting with a lower mantle shear velocity discontinuity or strong vertical gradient [*Young and Lay*, 1987] while S^{SV} is not. *Lay and Young* [1991], *Matzel et al.* [1996], and *Garnero and Lay* [1997] showed similar waveform characteristics for S waves propagating through the lowermost mantle beneath Alaska.

3. Modeling of T_{SSV_SSH} times

Figure 3 shows T_{SSV_SSH} measurements obtained by estimating time shifts necessary to match the upswing of the S^{SH} and S^{SV} wave signals. T_{SSV_SSH} values scatter about zero between 71° and 80° (data from events A and B) while T_{SSV_SSH} is larger than +2 s at epicentral distances greater than 87° (data from event C). T_{SSV_SSH} predictions for three sets of shear velocity models are also shown. These predictions are determined in a similar manner as the data using S^{SV} and S^{SH} waveform synthetics computed separately for different isotropic 1–D V_{SV} and V_{SH} profiles (Figure 4). These velocity profiles are simple deviations from model SYL1 [*Young and Lay*, 1987]. V_{SH} in model class I increases discontinuously at a depth of 2610 km (280 km above the CMB). Following *Garnero and Lay* [1997], shear velocity anisotropy is incorporated by in-

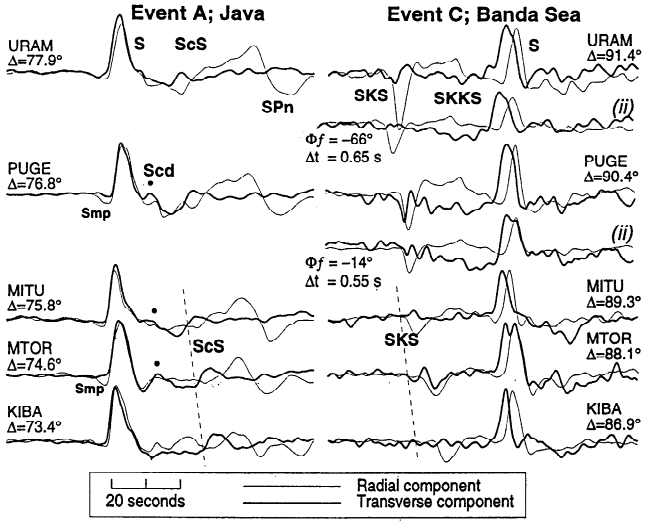

Figure 2. Shear wave recordings of events A and C at five stations of the Tanzania Network. The recordings are aligned on the S arrival time (PREM) and have a duration of 90 s. The thick and thin lines are the radial and transverse component recordings, respectively. Station codes and corresponding epicentral distances (Δ) and the phase names of several high–amplitude signals are plotted above the recordings. Recordings of event C at URAM and PUGE indicated by *(ii)* have been corrected for upper mantle anisotropy using the formalism of *Silver* [1996].

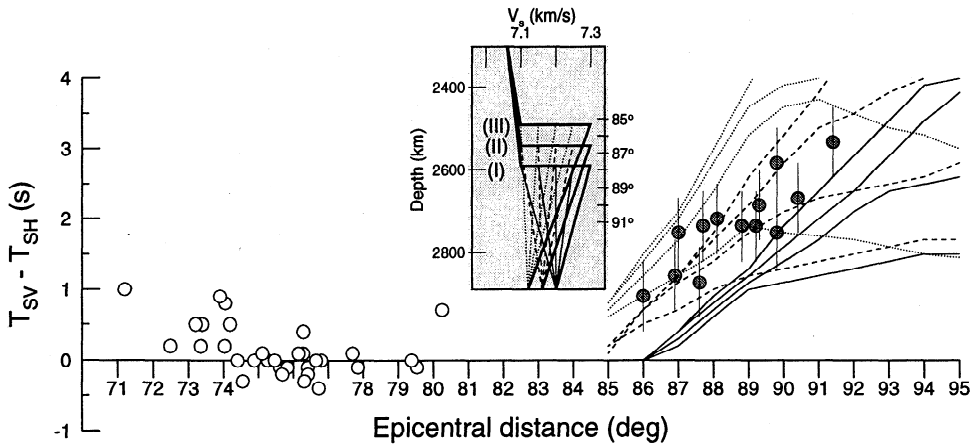

Figure 3. Measurements of T_{SSV_SSH} for events A and B (open circles) and event C (solid circles) as a function of epicentral distance. Predictions of T_{SSV_SSH} are computed for three classes of models, each incorporating four shear velocity profiles. In models of class I (solid lines), V_{SH} increases discontinuously by 2.8% at 2610 km depth. V_{SV} jumps at 2610 km are 0%, 0.7%, 1,4%, and 2.1%. In models of class II (dashed lines) and III (dotted lines), V_{SH} and V_{SV} discontinuously increase at 2540 km and 2491 km depth, respectively. The velocity profiles of these models are shown in the plot inserted in the middle of this Figure. Thick solid lines represent the V_{SH} profiles of models I, II, and III. while thin solid, dashed, and dotted lines represent V_{SV} profiles of model groups I II, and III, respectively. Tick marks on the right indicate S wave turning depths (using PREM).

voking smaller (0, 0.7%, 1.4% and 2.1%) discontinuous jumps of V_{SV}. Below this depth, V_{SH} and V_{SV} decrease monotonously with depth. In models of classes II and III, V_{SH} and V_{SV} discontinuities are at depths of 2540 km (350 km above the CMB) and 2491 km (400 km above the CMB), respectively.

T_{SSV_SSH} computed for these models increases systematically with epicentral distance as S waves propagates an increasingly larger distance through anisotropic structure in the lowermost mantle. The increase is strongest for models with the smallest V_{SV} increase at the lower mantle discontinuity (i.e., stronger shear velocity anisotropy). The minimum distance at which T_{SSV_SSH} is larger than zero value decreases when the onset of shear velocity anisotropy is placed shallower in the mantle.

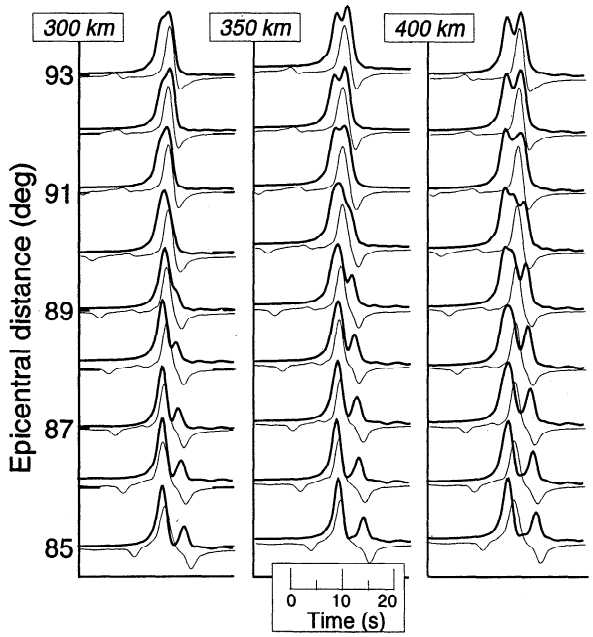

Figure 4. Transverse (thick lines) and radial (thin lines) seismograms computed separately for different V_{SH} and V_{SV} shear velocity profiles. In these models, V_{SV} and V_{SH} increase discontinuously by 1.4% and 2.8%, respectively, at 300 km (left), 350 km (middle), and 400 km (right) above the CMB.

Model class I predictions underestimate the observed values of T_{SSV_SSH} for either magnitude of the V_{SV} jump. This indicates that shear velocity anisotropy must be present at depths shallower than 2610 km in order to match the large values of T_{SSV_SSH} at 88°. Model classes II and III, which invoke V_{SV} and V_{SH} jumps 50 to 100 km higher in the mantle, provide a better match to the data. In order to reproduce the increase of T_{SSV_SSH} with epicentral distance, the jump in V_{SV} is constrained to be about two to three times smaller than the V_{SH} jump. A smaller jump in V_{SV} results in an increase of T_{SSV_SSH} faster than observed. The significant scatter in T_{SSV_SSH} and the short epicentral distance range spanned by the data preclude placing more stringent constraints.

4. Discussion and Conclusions

Various mechanisms underlying the cause of shear velocity anisotropy in D" have been proposed. *Kendall and Silver* [1998], *Lay et al.* [1998a], and *Karato* [1998] provide extensive reviews of these mechanisms. Shear velocity anisotropy can be produced by horizontally laminated structures such as melted former–oceanic crust [*Kendall and Silver*, 1996], core–mantle boundary reaction products [*Pulliam and Sen*, 1998], and partial melt associated with the ultra–low velocity zone in the low-

ermost mantle [*Lay et al.*, 1998b]. Alternatively, lattice preferred orientation of, predominantly, (Mg,Fe)O may be involved [e.g., *Karato*, 1998]. Each mechanism suggest the influence of horizontal shear of lowermost mantle material associated with descending slabs and is possibly enhanced by a transition to a dislocation creep deformation in D", as a result of the relatively high temperatures in D" [e.g., *Lay et al.*, 1998a].

Seismic shear velocity anisotropy beneath the Indian Ocean is characterised by positive values of T_{SSV_SSH}, consistent with transverse isotropy with a vertical symmetry axis. Values of T_{SSV_SSH} of 2 s at distances as short as 88° indicate that anisotropic structure is present at least 350 km above the core–mantle boundary. Because of the significant scatter, the magnitude, $\eta = 1 - V_{sv}/V_{sh}$, is uncertain but 1.4% and 2.7% represent lower and upper bounds. The variation of shear velocity anisotropy is also poorly constrained because of the limited epicentral distance span provided by the Tanzania network.

SKKS coda, S–to–p converted phases at the Moho, and upper mantle heterogeneity beneath the stations obscure the onset of S^{SV} and complicate wave shapes. Hence, it is difficult to infer whether azimuthal anisotropy needs to be invoked in the model.

Acknowledgments. All figures were generated with the GMT software of P. Wessel and W. H. F. Smith. The IRIS/DMC provided the Tanzania data. This research is funded by NSF grant EAR98–96210. Contribution 8674 of the Division of Geological and Planetary Sciences, California Institute of Technology.

References

Dziewonski, A. M., and D. L. Anderson, Preliminary reference Earth model, *Phys. Earth Plan. Inter.*, *25*, 297–356, 1981.

Dziewonski, A. M., G. Ekström, and X.-F. Liu, Structure at the top and bottom of the mantle, in *Monitoring a Comprehensive Test Ban Treaty*, E.S. Husebye and A. M. Dainty (eds), Kluwer Ac. Publ., pp. 521–550, 1996.

Garnero, E., and T. Lay, Lateral variations in lowermost mantle shear velocity anistropy beneath the north Pacific and Alaska, *J. Geophys. Res.*, *102*, 8121–8135, 1997.

Hill, A. A., T. J. Owens, J. Ritsema, A. A. Nyblade, and C. A. Langston, Constraints on the upper mantle structure beneath the Tanzania craton from teleseismic body waves, *Eos, Trans. AGU Suppl.*, *77*, F477, 1996.

Karato, S.-I., Some remarks on the origin of seismic anisotropy in the D" layer, *Earth Planets Space*, *50*, 1019–1028, 1998.

Kendall, J.-M., and P. G. Silver, Constraints from seismic anisotropy on the nature of the lowermost mantle, *Nature*, *381*, 409–412, 1996.

Kendall, J.-M., and P. G. Silver, Investigating causes of D" anisotropy, in *The core–mantle boundary region; Geodyn. Ser. 28*, M. Gurnis, M. E. Wysession, E. Knittle, and B. A. Buffett, Eds., American Geophysical Union, Washington DC, pp. 97–118, 1998.

Lay, T. and C. J. Young, Analysis of seismic SV waves in the core's penumbra, *Geophys. Res. Lett.*, *18*, 1373–1376, 1991.

Lay, T., Q. Williams, E. J. Garnero, L. Kellogg, and M. E. Wysession, Seismic wave anisotropy in the D" region and its implications, in *The core–mantle boundary region; Geodyn. Ser. 28*, M. Gurnis, M. E. Wysession, E. Knittle, and B. A. Buffett, Eds., American Geophysical Union, Washington DC, pp. 299–318, 1998a.

Lay, T., Q. Williams, and E. J. Garnero, The core–mantle boundary layer and deep Earth dynamics, *Nature*, *392*, 461–468, 1998b.

Matzel, E., M. Sen, and S. Grand, Evidence for anisotropy in the deep mantle beneath Alaska, *Geophys. Res. Lett.*, *23*, 2417–2420, 1996.

Nyblade, A. A., Birt, C., Langston, C. A., Owens, T. J., and R. Last, Seismic experiment reveals rifting of craton in Tanzania, *Eos Trans. AGU*, *77*, 517–521, 1996.

Pulliam, J., and M. K. Sen, Seismic anisotropy in the core–mantle transition zone, *Geophys. J. Int.*, *135*, 113–128, 1998.

Ritsema, J., E. Garnero, T. Lay, and H. Benz, Seismic anisotropy in the lowermost mantle beneath the Pacific *Geophys. Res. Lett.*, *25*, 1229–1232, 1998.

Ritsema, J., A. A. Nyblade, T. J. Owens, C. A. Langston, and J. C. VanDecar, Uppermantle seismic velocity structure beneath Tanzania: implications for the stability of cratonic lithosphere, *J. Geophys. Res.*, *103*, 21,201–21,213, 1998.

Ritsema, J., and H. van Heijst, New seismic model of the upper mantle beneath Africa, *Geology*, *28*, 63–66, 2000.

Russel, S. A., T. Lay, and E. J. Garnero, Seismic evidence for small–scale dynamics in the lowermost mantle at the root of the Hawaiian hotspot, *Nature*, *396*, 255–258, 1998.

Silver, P. G., Seismic anisotropy beneath continents: Probing the depth of geology, *Annu. Rev. Earth Planet. Sci.*, *24*, 385–432, 1996.

Van Heijst, H. J., J. Ritsema, and J. Woodhouse, Global P and S velocity structure derived from normal mode splitting, surface wave dispersion, and body wave travel time data, *Eos, Trans. AGU Suppl.*, *80*, S221, 1999.

Vinnik, L., B. Romanowicz, Y. LeStunff, L. Makeyeva, Seismic anisotropy in the D" layer, *Geophys. Res. Lett.*, *22*, 1657–1660, 1995.

Young, C. J., and T. Lay, Evidence for a shear velocity discontinuity in the lowermost mantle beneath India and the Indian Ocean, *Phys. Earth Planet. Inter.*, *49*, 37–53, 1987.

J. Ritsema, Seismological Laboratory 252–21, California Institute of Technology, Pasadena, CA 91125, USA.

(Received September 9, 1999; revised January 21, 2000; accepted February 20, 2000.)